Modulation of the Redox Potentials of FMN in *Desulfovibrio vulgaris* Flavodoxin: Thermodynamic Properties and Crystal Structures of Glycine-61 Mutants[†,‡]

Paul A. O'Farrell,[§] Martin A. Walsh,[||,⊥] Andrew A. McCarthy,[||] Timothy M. Higgins,[||] Gerrit Voordouw,[#] and Stephen G. Mayhew*[,§]

Department of Biochemistry, University College Dublin, Belfield, Dublin 4, Ireland, Department of Chemistry, University College Galway, Ireland, European Molecular Biology Laboratory (EMBL), c/o DESY, Notkestrasse 85, D-22603 Hamburg, Germany, Department of Biological Sciences, University of Calgary, Alberta, Canada

Received December 31, 1997; Revised Manuscript Received March 16, 1998

ABSTRACT: Mutants of the electron-transfer protein flavodoxin from *Desulfovibrio vulgaris* were made by site-directed mutagenesis to investigate the role of glycine-61 in stabilizing the semiquinone of FMN by the protein and in controlling the flavin redox potentials. The spectroscopic properties, oxidation−reduction potentials, and flavin-binding properties of the mutant proteins, G61A/N/V and L, were compared with those of wild-type flavodoxin. The affinities of all of the mutant apoproteins for FMN and riboflavin were less than that of the wild-type apoprotein, and the redox potentials of the two 1-electron steps in the reduction of the complex with FMN were also affected by the mutations. Values for the dissociation constants of the complexes of the apoprotein with the semiquinone and hydroquinone forms of FMN were calculated from the redox potentials and the dissociation constant of the oxidized complex and used to derive the free energies of binding of the FMN in its three oxidation states. These showed that the semiquinone is destabilized in all of the mutants, and that the extent of destabilization tends to increase with increasing bulkiness of the side chain at residue 61. It is concluded that the hydrogen bond between the carbonyl of glycine-61 and N(5)H of FMN semiquinone in wild-type flavodoxin is either absent or severely impaired in the mutants. X-ray crystal structure analysis of the oxidized forms of the four mutant proteins shows that the protein loop that contains residue 61 is moved away from the flavin by 5−6 Å. The hydrogen bond formed between the backbone nitrogen of aspartate-62 and O(4) of the dimethylisoalloxazine of the flavin in wild-type flavodoxin is absent in the mutants. Reliable structural information was not obtained for the reduced forms of the mutant proteins, but if the mutants change conformation when the flavin is reduced to the semiquinone, to facilitate hydrogen bonding between N(5)H and the carbonyl of residue 61, then the change must be different from that known to occur in wild-type flavodoxin.

Flavodoxins are small flavoproteins isolated from a variety of microorganisms and eukaryotic algae that contain a molecule of FMN and that function as electron carriers in reactions of low oxidation−reduction potential (*1*−*3*). They stabilize the flavin semiquinone and cause a large negative shift in the oxidation−reduction potential for the 1-electron reduction of the semiquinone to the hydroquinone to a potential that is in the range −0.372 V to −0.518 V. These observations led to the view that when flavodoxins operate in low-potential reactions, they function as 1-electron carriers that cycle between the semiquinone and hydroquinone without direct involvement of the oxidized form of the flavin. Much recent work has sought to explain how the apoprotein of flavodoxins modifies the properties of FMN to allow the bound flavin to function in this way.

Spectroscopic measurements have shown that the dimethylisoalloxazine moiety of the flavin of flavodoxins is neutral in the oxidized and semiquinone forms. The p*K* at 8.5 associated with N(5)H of the semiquinone of free FMN is raised to at least p*K* 13 in the complexes with flavodoxins from *Megasphaera elsdenii* and *Clostridium beijerinckii* (*1*−*4*). The hydroquinone is present as the anion (*5*−*8*). Therefore the two 1-electron redox steps for flavodoxins, with the associated oxidation−reduction potentials E_2 and E_1, can be represented as follows:

$$\mathrm{FMN} + \mathrm{e}^- + \mathrm{H}^+ \overset{E_2}{\longleftrightarrow} \mathrm{FMNH}^\bullet \quad (1)$$

$$\mathrm{FMNH}^\bullet + \mathrm{e}^- \overset{E_1}{\longleftrightarrow} \mathrm{FMNH}^- \quad (2)$$

The complex of protein and flavin in the flavodoxins is very strong but noncovalent, with a dissociation constant (K_d) for the oxidized complex of 1 nM or less (*1*−*3*). Values for

[†] This work was supported by Forbairt and the European Commission through the Human Capital and Mobility Program (CHRX-CT93-0166). M.A.W. was supported by an EC Institutional Fellowship (CT 930485).

[‡] The coordinates and structure factors for the structures described above have been deposited with the Brookhaven Protein Data Bank with the reference codes 1akr, 1azl, 1akw, and 1akt for the coordinates of G61A, G61V, G61L, and G61N, respectively, and r1akrsf, r1azlsf, r1akwsf, and r1aktsf, respectively, for the corresponding structure factors.

* To whom correspondence should be addressed. Phone: 353 1 7061572. Fax: 353 1 2837211. E-mail: Stephen.G.Mayhew@UCD.IE.

[§] University College Dublin.

[||] University College Galway.

[⊥] European Molecular Biology Laboratory.

[#] University of Calgary.

S0006-2960(97)03193-0 CCC: $15.00 © 1998 American Chemical Society
Published on Web 05/20/1998

the dissociation constants of the complexes of the two reduced forms of FMN have been calculated using the K_d value for the oxidized complex and the differences in the redox potentials between the free and bound flavin. The calculations reveal that the semiquinone is bound to the protein very much more strongly than the oxidized flavin, while the flavin hydroquinone is bound relatively weakly. Recent studies with mutants of flavodoxin from *Desulfovibrio vulgaris* have suggested that the low stability of the hydroquinone complex results from charge repulsion between the negative charge on the dimethylisoalloxazine moiety of the flavin in this redox state and negative charges on the protein, and also from unfavorable aromatic stacking interactions between the flavin hydroquinone and the side chain of a tyrosine residue that flanks the *si* face of the dimethylisoalloxazine (*9*−*12*). An early suggestion that the hydroquinone might be destabilized because it is held almost flat by the protein, while it is bent in free flavin, was discarded when NMR measurements on free flavin hydroquinones indicated that they too are flat (*13*). Nevertheless theoretical calculation suggests that the neutral hydroquinone of free flavin is in fact bent along the N(5)−N(10) axis with a puckering angle of 26.5° but with a low energy barrier to inversion (<6.5 kcal mol^{-1} (*14*)).

Comparison of the three-dimensional structures of flavodoxins from *C. beijerinckii* (*15*), *D. vulgaris* (*16*), *Anacystis nidulans* (*17*), *Desulfovibrio desulfuricans* (*18*), and *M. elsdenii* (*19, 20*) in their oxidized states with the corresponding structures in at least one of the two reduced states has shown that a new hydrogen bond forms between N(5)H of the reduced flavin and a backbone carbonyl group of the protein. In all but the last of these flavodoxins, a change in the protein conformation accompanies reduction of the flavin. It was proposed that the new hydrogen bond might help to stabilize the protein−semiquinone complex relative to the oxidized form of the complex (*15*). The carbonyl group is provided by glycine residues in flavodoxins from *C. beijerinckii*, *D. vulgaris*, *D. desulfuricans*, and *M. elsdenii*, but by an asparagine in the flavodoxin from *A. nidulans* (an asparagine also occurs at the corresponding position in the sequence of flavodoxin from *Chondrus crispus*). The redox potentials for the reduction of oxidized flavodoxin to the semiquinone at pH 7 fall in the range −41 mV to −143 mV for the first group of flavodoxins (compared with −238 mV for FMN (*21*)), while the corresponding potential for *A. nidulans* flavodoxin (−221 mV) is much closer to that of the free flavin. It was suggested that the conformational change associated with reduction of *A. nidulans* flavodoxin might be hindered by the bulky side chain of the asparagine that provides the carbonyl for the hydrogen bond (*22*). To test this idea with *D. vulgaris* flavodoxin, the corresponding glycine residue (Gly61) was replaced by asparagine (*23*). The semiquinone of the mutant was found to be less stable than the semiquinone in wild-type *D. vulgaris* flavodoxin. We have now made additional mutants to change the size of the side chain at this position, and to compare the thermodynamic and other properties of the mutant proteins with those of the wild-type protein. The three-dimensional structures of the oxidized forms of the four mutants have been determined by X-ray crystallography.

METHODS AND MATERIALS

Mutagenesis, Gene Expression, and Purification of Proteins. The gene for flavodoxin is contained in the 554-bp *Eco*RI-*Hin*dIII insert pFl300 (*24*). Site-directed mutagenesis was carried out by the method of Kunkel et al (*25*) as described by Carr et al (*23*). However, the gene was found to be unstable when it was carried as an insert in the M13 vector, and to be either completely deleted or to lose the region that codes for the C-terminal half of the protein. It was therefore restricted at the *Pst*I site close to the center of the gene (*24*), and the two fragments were used to make two new vectors: M13 mpEP300 that contained the sequence from the *Eco*RI site, including the ribosome-binding site, up to the internal *Pst*I site, and M13 mpPH300 coding for the C-terminal half of the protein, from the *Pst*I site to the *Hin*dIII site. Mutagenesis was then carried out using mpEP300, the part of the gene that codes for the N-terminal region of the protein. A degenerate oligonucleotide, 5′A GTG GTG A(GA)(GC) CCA CGT CG, obtained from the Regional DNA Synthesis Laboratory, University of Calgary, was used for mutagenesis. Single-stranded DNA isolated from potential mutants was sequenced (*26*) to identify the mutation. The complete gene was then reconstructed, and it was cloned into the expression vector *pDK*6 (*27*), as used earlier to obtain expression of the wild-type protein (*24*).

The genes for the three new mutant flavodoxins, G61A, G61V, and G61L, were expressed in *Escherichia coli* TG2, as described for the wild-type gene (*24*) except for the bacterial growth medium which was Terrific Broth (*28*). The mutant proteins were purified from crude extracts as described for recombinant wild-type protein (*24*).

Determination of Absorption Coefficients and Dissociation Constants for the Complexes of Mutant Apoflavodoxins with FMN or Riboflavin. Values for the absorption coefficients of oxidized mutant flavodoxins were determined by spectrophotometric titration of FMN with excess of mutant apoflavodoxin, made by extraction of the holoprotein with trichloroacetic acid (*29*). The FMN used was also obtained from flavodoxin (*30*). Dissociation constants for the complexes of mutant apoflavodoxins with FMN and riboflavin were determined by fluorometric and spectrophotometric titration respectively (*24, 29*). A value for the absorption coefficient of the semiquinone of the G61A mutant at the maximum at 577 nm was determined from a stepwise photoreduction of the flavoprotein with EDTA as the photooxidizable substrate and 3-methyl-5-deazalumiflavin as the catalyst (*31*). The plot of $A_{577\ nm}$ versus $A_{462\ nm}$, an absorption maximum in the oxidized protein, gave two linear regions which were extrapolated to their point of intersection; the intersection point gave an absorption coefficient of 4.55 mM^{-1} cm^{-1} at 577 nm for fully formed semiquinone. This extrapolation could not be made with the corresponding plots for the G61V and G61L mutants because relatively little semiquinone was formed during the photoreduction and the plots did not have linear sections; an absorption coefficient of 4700 M^{-1} cm^{-1} at 580 nm, similar to that of the wild-type protein, was assumed.

Determination of Oxidation−Reduction Potentials. Values for the two oxidation−reduction potentials of the mutant flavodoxins were determined by potentiometry with a Sycopel DP 301/S potentiostat and an anaerobic spectroelec-

trochemical cell similar to that described by Stankovich (*32*). The flavodoxin in the cell was reduced electrolytically, or photochemically as described above. The following dyes were used to mediate electron transfer between the protein-bound flavin and the gold plate used as the sensing electrode: benzyl viologen, neutral red, saffranine T, or rosinduline, all at 1 μM; when electrochemical reduction was used, 1,1′-trimethylene-2,2′-bipyridylium (triquat) was added to 100 μM to carry reducing equivalents from a second gold plate used as the working electrode. After each period of reduction, the system in the cell was allowed to equilibrate until $\Delta A_{580} < 0.001$ and $\Delta E_h < 1$ mV in 20 min (where E_h is the potential versus the standard hydrogen electrode). In the case of the G61A mutant, plots were made of the observed potential, E_h, versus ln([Fl]/[FlH$^\bullet$])[1] for the first step in the reduction (where Fl and FlH$^\bullet$ are the oxidized and semiquinone forms of flavodoxin), and of E_h versus ln([FlH$^\bullet$]/FlH$^-$]) for the second step (where FlH$^-$ is the anion of the hydroquinone of flavodoxin). Values for midpoint potentials E_2 and E_1 for the first and second steps, respectively, in the reduction were calculated from these plots. Data obtained for E_2 at different pH values were fitted to a straight line using MacCurveFit. The same program was used to fit data obtained for E_1 at different pH values; the data were fitted to a theoretical curve for a redox system in which the reductant protonates.

The semiquinone forms of the G61V and G61L mutants have much less thermodynamic stability than the semiquinones of wild-type protein and the G61A mutant, with the result that all three redox forms of these two mutants are present at all stages of reduction, and a different method of calculation was therefore used to determine their midpoint potentials. The concentration of the semiquinone is at a maximum at 50% reduction of flavodoxin and its mutants, due to the equilibrium:

$$2\mathrm{FlH}^\bullet = \mathrm{Fl} + \mathrm{FlH}^- \tag{3}$$

The concentration of semiquinone was determined from the absorbance at 580 nm, a wavelength at which only the semiquinone absorbs, and the apparent semiquinone formation constant for the equilibrium ($K_{app} = [\mathrm{FlH}^\bullet]^2/[\mathrm{Fl}][\mathrm{FlH}^-]$) was calculated using eq 4:

$$\sqrt{K_{app}} = \frac{2[\mathrm{FlH}^\bullet]_{max}}{([\mathrm{Fld}] - [\mathrm{FlH}^\bullet]_{max})} \tag{4}$$

where K_{app} is the apparent semiquinone formation constant at a given pH, $[\mathrm{FlH}^\bullet]_{max}$ is the concentration of semiquinone at 50% reduction, and [Fld] is the total concentration of all species of flavodoxin (*33*).

Equations 5−8, adapted from Michaelis (*34*), then allow the concentrations of the oxidized and hydroquinone forms of flavodoxin to be determined from the observed concentration of semiquinone at all stages of the reduction,

$$x = [\mathrm{Fld}] \pm \sqrt{[\mathrm{Fld}] - 2[\mathrm{FlH}^\bullet][\mathrm{Fld}] + \frac{4[\mathrm{FlH}^\bullet]^2}{K_{app}} - [\mathrm{FlH}^\bullet]^2} \tag{5}$$

where x is the degree of oxidation ($x = 2$, 1, and 0 for fully oxidized, semiquinone, and fully reduced, respectively), [Fld] is the total concentration of all species of flavodoxin, [FlH$^\bullet$] is the concentration of semiquinone, and K_{app} is the apparent semiquinone formation constant. The positive root is used when $x > 1$ and the negative root when $x < 1$. The equation is valid only when $K_{app} < 4$.

$$[\mathrm{Fl}] = [\mathrm{Fld}]\frac{p}{2} + \frac{x}{2} - \frac{1}{2}\sqrt{Y} \tag{6}$$

$$[\mathrm{FlH}^-] = [\mathrm{Fld}]\left(1 + \frac{p}{2}\right) - \frac{x}{2} - \frac{1}{2}\sqrt{Y} \tag{7}$$

where [Fl] is the concentration of oxidized flavodoxin, [FlH$^-$] is the concentration of the hydroquinone,

$$p = \frac{K_{app}}{4 - K_{app}}, \text{ and } Y = p^2([\mathrm{Fld}])^2 + 2x[\mathrm{Fld}] - px^2$$

A plot was made of E_h versus ln([Fl]/[FlH$^-$]) to determine the midpoint potential (E_m) for the overall 2-electron reduction of flavodoxin to the hydroquinone. The value for $E_2 - E_1$ in volts was calculated from K_{app} using eq 8, allowing values for E_2 and E_1 to be calculated.

$$E_2 - E_1 = 0.059\log_{10}K_{app} \tag{8}$$

This method requires a value for the absorption coefficient of the semiquinone at about 580 nm, and as this could not be determined directly for G61V and G61L, an assumed value of 4.7 mM^{-1} cm^{-1} was used. However, when the semiquinone formation constant is between 0.1 and 4, even a substantial error in the value for absorption coefficient leads to only a small error in the values calculated for the two redox potentials. For example, when the value assumed for the absorption coefficient was varied in the range 4−5.3 mM^{-1} cm^{-1}, the values calculated for E_1 and E_2 deviated by only ±6 mV. This deviation is small compared with the large change in the potentials that occurs when wild-type protein undergoes these two mutations.

Crystallization, Data Collection, and Processing. Native flavodoxin and the wild-type recombinant protein crystallize readily from 65% to 75% saturated ammonium sulfate in a number of buffering solutions and over a wide pH range as yellow bipyramids in the tetragonal space group $P4_32_12$ (*35*, *36*). The mutant proteins did not crystallize as easily. Trials using the hanging-drop vapor diffusion method at 4 and 18 °C failed to give crystals using ammonium sulfate with Tris-HCl buffers in the pH range 7−7.5. However, bunches of needlelike crystals were obtained when acetone was added (1−2% v/v final concentration) to solutions of protein in 10 mM Tris-HCl buffer, pH 7.0, 1 mM EDTA, and 60−70% saturated ammonium sulfate at 18 °C. Crystals isolated from these bunches were used to seed hanging drops that had been prepared by mixing 4 μL of protein (15 mg/mL) in 10 mM Tris buffer, pH 7.0, and 1 mM EDTA with 4 μL of 60−70% saturated ammonium sulfate and that had been allowed

[1] Abbreviations: Fl, oxidized flavodoxin; FlH$^\bullet$, flavodoxin semiquinone; FlH$^-$, flavodoxin hydroquinone; Fld, flavodoxin (all redox forms); ox, oxidized; sq, semiquinone; hq, hydroquinone.

Table 1: Unit Cell Parameters for Crystals of G61 Mutant Proteins

G61 mutant	space group	dimension (Å)		
		a	*b*	*c*
alanine	$P2_12_12$	56.49	87.99	35.08
valine	$P2_12_12$	56.60	88.12	35.19
leucine	$P2_12_12$	56.93	88.61	35.42
asparagine	$P2_12_12$	56.14	87.58	34.99
wild type	$P4_32_12$	51.6	51.6	139.5

to equilibrate for 2−3 days. The seed crystals grew in size over 2−3 weeks and the seeding procedure was then repeated several times until the crystals reached a suitable size for X-ray diffraction data collection. The crystals form as orange blocks and they belong to the orthorhombic space group $P2_12_12$ (Table 1).

Crystals were mounted in glass capillaries using standard procedures (*37*), and data were collected at 4 °C using synchrotron radiation on a MAR Research Imaging plate scanner. Details of the data collection for the four mutants are listed in Table 2. Two sets of data were collected from the G61A and G61L crystals at resolution cutoffs of 1.47 and 3.2 Å (G61A) and 1.62 and 3.2 Å (G61L) to avoid saturation of the high-intensity low-angle reflections. Single data sets were used for the G61N and G61V mutants. The reflection intensities were integrated, merged, and scaled using the programs DENZO and SCALEPACK (*38*). The quality of the data is reported in Table 2.

Structure, Solution, and Refinement. Molecular replacement was performed with the MERLOT suite (*39*) using intensity data from G61V in the range 8−4 Å. The search model used was a 2.5 Å refined structure of wild-type *D. vulgaris* flavodoxin (*35*). This structure is almost identical to the structure at 1.9 Å of the P2A mutant protein studied by Watt et al. (*16*).

The cross rotation function gave only one significant peak (9σ) at $\theta1 = 170$, $\theta2 = 55$, $\theta3 = 190$. The Crowther and Blow translation function gave a clear solution at $x = 0.350$, $y = 0.345$, $z = 0.139$. The crystallographic *R* factor after molecular replacement was 41.5%. After rigid body refinement with the program RMINIM (*39*), the *R* factor decreased to 38.7%.

Refinement of the structures was carried out by restrained least-squares minimization using the CCP4 (*40*) Fast Fourier version of PROLSQ (*41*). All data were used (no σ cutoff) from 10 Å to the high resolution limit of each data set (Table 2). Modeling of solvent sites was executed with an automatic refinement program (ARP) (*42*) which models and updates solvent structure after each refinement cycle. Only potential water sites within 2.2−3.3 Å of existing atoms in the model were considered. In the refinement of the G61A, G61L, and G61N mutants, 5% of the data was set aside for use as a cross validation set (*43*).

A description follows of the refinement of the data for the G61V mutant, the first mutant to be refined. After 10 cycles of least-squares minimization, the *R* factor decreased to 27%. The model was inspected with $3F_o - 2F_c$ and $F_o - F_c$ electron density maps using the program O (*44*).. Electron density at the mutation site was unclear, and to aid rebuilding and to reduce model bias, five cycles of refinement were carried out with residues 60−70 omitted from the refinement. This region of the structure was then manually rebuilt and refinement continued. Solvent sites were then automatically located after each cycle of PROLSQ with the program ARP. The refinement continued with manual rebuilding of the model until it converged after the addition of 126 waters to an *R* factor of 17.5%.

The refined coordinates of the G61V structure without the solvent molecules were used to start refinement of the G61A, G61L, and G61N structures. Refinement of these structures followed a similar trend to that described above. The refinements converged to final *R* factors of 18.4%, 17.1% and 18.1%, for G61A, G61L, and G61N, respectively. The final statistics for the refined models are reported in Table 3. An ensemble Ramachandran plot (*45*) of wild-type flavodoxin and the G61A mutant is shown in Figure 1. For the mutant, 90.3% of the residues are located in the most favored regions, 9.7% are in the additional allowed regions, and none occur in the generously allowed and disallowed regions of the plot. In contrast, Asp62 in wild-type flavodoxin is found in a disallowed region. The electron density for the 60 loop and FMN in the G61A mutant which was refined against data extending to 1.58 Å is shown in Figure 2. Similar high-quality electron density is observed for most of the structure. The other mutants also have well-defined density for most of the structure. The electron density for the mutated residue is clear for all of the structures except that in the G61N mutant, for which the electron density is poor. The asparagine residue in this mutant is partially disordered although some electron density is visible at the 0.5σ for the side chain atoms past the Cβ carbon.

RESULTS

Purification and General Properties of the Mutant Proteins. The level of expression of the mutant proteins was similar to that of wild-type recombinant flavodoxin (*24*). The purified proteins gave single bands after SDS−PAGE analysis, and the electrophoretic mobility of the mutants was the same as that of wild-type protein. The absorption spectra of the oxidized forms of the mutant proteins are similar to that of wild-type flavodoxin with three maxima in the UV−visible region. Differences from the wild-type protein occur in the wavelengths and absorption coefficients at the maxima for the mutants, implying that structural changes have

Table 2: X-ray Crystallography Data Collection and Processing Statistics

G61 mutant	resolution range (Å)	observations	unique reflections	completeness[a] (%)	R_{merge}[b] (%)
alanine	1.58	126 829	24 403	98.9 (87.6)	3.6 (34.1)
valine	1.80	87 934	19 560	98.0 (82.6)	5.9 (44.1)
leucine	1.75	110 226	18 715	99.8 (96.4)	4.6 (33.7)
asparagine	1.80	50 204	14 539	88.0 (86.7)	2.6 (27.8)

[a] Values in parentheses are for the highest-resolution shell. [b] $R_{merge} = \sum_{hkl}\sum_{i=1}^{N}|\langle I^{hkl}\rangle - I_i^{hkl}|/\sum_{hkl}\sum_{i=1}^{N} I_i^{hkl}$.

Table 3: Refinement Statistics

	G61A	G61V	G61L	G61N
resolution (Å)	10−1.58	10−1.80	10−1.75	10−1.8
R factor[a]	18.4	17.5	17.1	18.1
free *R* factor[b]	20.6		19.4	21.3
atoms (nonhydrogen)				
total	1246	1263	1238	1241
protein	1105	1106	1108	1108
FMN	31	31	31	31
water	110	126	99	102
rms deviations from ideal geometry (Å)				
bond distance (1−2)	0.009	0.016	0.01	0.01
angle distance (1−3)	0.03	0.045	0.035	0.041
planar distance (1−4)	0.033	0.044	0.036	0.041
mean displacement parameters (Å^2)				
all atoms	27.6	23.5	26.4	23.9
protein atoms	26.0	21.4	25.0	22.6
FMN atoms	16.4	13.8	16.2	14.7
solvent atoms	46.9	43.2	45.0	40.5

[a] $R = 100\ \sum_h|F_o - F_c|/\sum_h|F_o|$. [b] Free *R* factor is calculated from 5% of the data which were omitted during the course of the refinement.

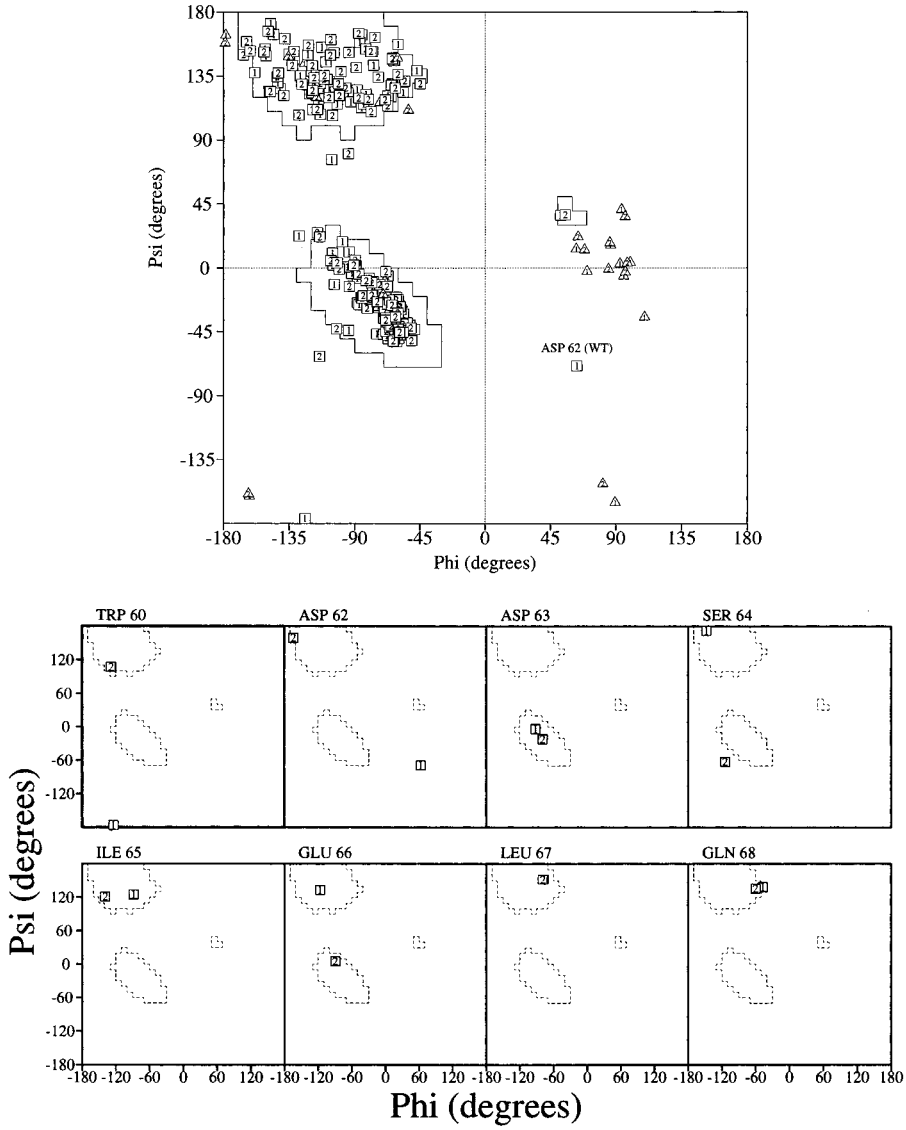

FIGURE 1: Upper plot: Ensemble Ramachandran plot for wild-type and G61A mutant flavodoxins. Residues in the wild-type protein are indicated by "1" and in the mutant by "2". Glycines are represented as triangles. Lower plot: Individual ensemble Ramachandran plots for residues 60−68 of the 60 loop in wild type and G61A mutant flavodoxins, labels as in upper plot. The figures were produced with the program Procheck (*58*).

occurred as a result of the mutations (Table 4, Figure 3). The ratio of absorbance of the maximum in the UV to the absorbance of the longest wavelength maximum in the visible region is higher for the three new mutants than for wild-

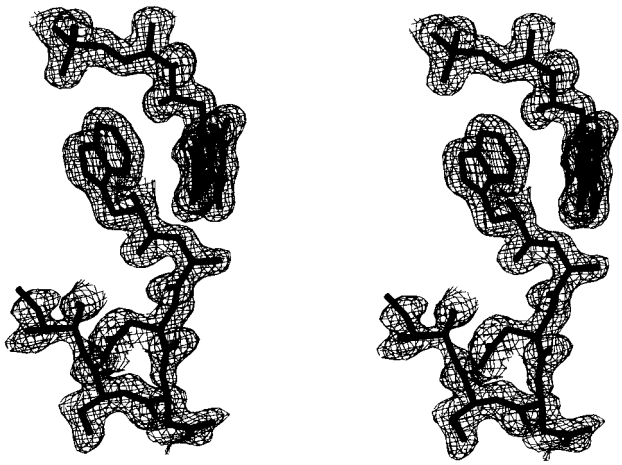

FIGURE 2: Stereoview of the final 3Fo − 2Fc electron density for the 60 loop and FMN of the G61A mutant flavodoxin. The electron density is contoured at the 1σ level.

type protein, due in part to their smaller absorption coefficients at the maximum in the visible region.

Oxidation−Reduction Properties. All of the Gly61 mutants are readily photoreduced, first to the semiquinone, and then to the hydroquinone. The light absorption spectra of the two reduced forms of each mutant protein are similar to those of wild-type flavodoxin. All of the mutants stabilize the semiquinone in its neutral blue form, as judged by the spectra at wavelengths greater than about 520 nm, but the extent of semiquinone formation depends on the mutant. About 99% of the flavin of wild-type flavodoxin is converted to the semiquinone after addition of one reducing equivalent at pH 7 (*24*); the corresponding value for G61A and G61N is about 80%, while for G61V and G61L only about 20% of the FMN is present as the semiquinone at half reduction due to extensive disproportionation according to the equilibrium of eq 3.

Aeration of solutions of fully reduced flavodoxin results in a very rapid formation of the semiquinone, followed by a slower reaction in which the fully oxidized protein forms. The oxidation of the hydroquinone by molecular oxygen involves a number of reactions, including the formation of superoxide (*1*). The conversion of semiquinone to fully oxidized flavodoxin is pseudo-first order. The fully reduced

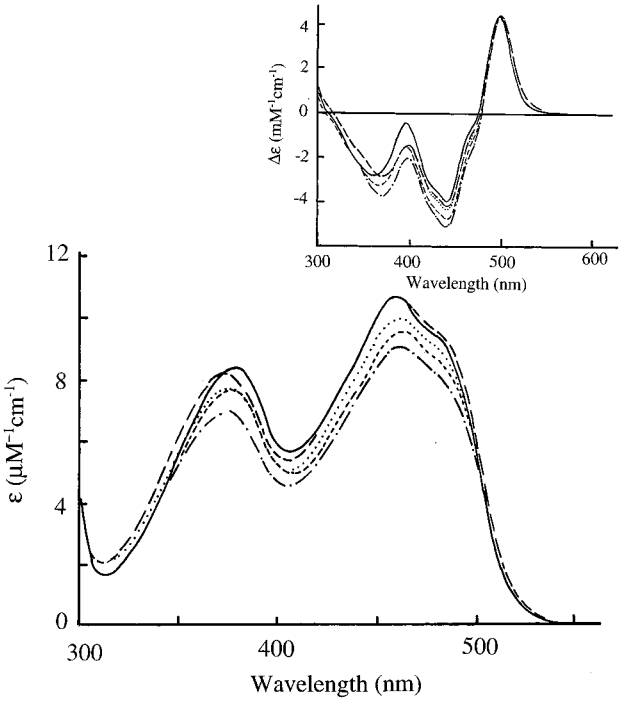

FIGURE 3: Absorption spectra of wild-type and glycine-61 mutant flavodoxins. The spectra were recorded in 50 mM K phosphate buffer pH 7 and 0.3 mM EDTA. The inset shows difference spectra measured between protein-bound FMN and free FMN: (−), wild-type; (− −), G61N; (···), G61L; (- - -), G61A; (− · −), G61V.

mutant flavodoxins react with oxygen in a qualitatively similar way. However the rate of reoxidation of the semiquinone of the G61A mutant (0.47 min^{-1}) is much greater at pH 7 than that of the semiquinone of the wild-type protein (0.0018 min^{-1} (*24*)), but slower than that for the G61N mutant (2.69 min^{-1} (*23*)). The hydroquinones of mutant proteins G61V and G61L react very rapidly with oxygen. When air was mixed with the hydroquinone of these mutants, A_{580} increased to a value that was up to twice the maximum observed during photoreduction, and it then decreased to 0 after a few seconds. The extent of the initial reaction suggests that the reaction of hydroquinone with oxygen is more rapid than the reaction in which the semiquinone disproportionates. As a result, a higher concentration of semiquinone is observed due to kinetic stabi-

Table 4: Spectroscopic Properties of Flavodoxin and Its Glycine-61 Mutants

protein		maxima (ϵ) nm (mM^{-1} cm^{-1})				isosbestic points (nm) ox/sq	isosbestic points (nm) sq/hq
wild type[a]	ox	273 (46.3)		378 (8.9)	458 (10.7)	368	330
	sq	354		494	580 (4.75)	506	433
	hq	357 (sh)[b]		452 (sh)			
G61N[c]	ox	272 (61.8)		373 (13.5)	458 (10.7)	359	323, 395
	sq	352	385	493	580 (5.2)	513	422
	hq	400 (sh)					
G61A	ox	273 (43.1)		378 (7.77)	462 (9.65)	364	319
	sq	380	463 (sh)	490	577 (4.55)	514	396
	hq	410 (sh)		423			
G61V	ox	273 (44.0)		376 (7.1)	461 (9.16)	nd[d]	
	sq				∼580		
	hq	350 (sh)		400 (sh)			
G61L	ox	274 (56.0)		376 (7.77)	461 (10.0)	nd	
	sq				∼580		
	hq	360 (sh)		410 (sh)			

[a] Data from ref 24. [b] sh, shoulder. [c] Data from ref 23. [d] nd, none detected because all three redox forms are present throughout the reduction.

Table 5: Comparison of Redox Potentials of Flavodoxin and Its Glycine-61 Mutants[a]

	potentials (mV)		
flavodoxin	E_1	E_m	E_2
wild type[b]	−440 ± 5	−303 ± 5	−143 ± 5
G61N[c]	−347	−298	−248
G61A	−359 ± 5	−311 ± 5	−262 ± 6
G61V	−299 ± 5	−316 ± 5	−333 ± 6
G61L	−302 ± 6	−320 ± 6	−338 ± 6
FMN[d]	−172 (−124)	−205 (−219)	−238 (−314)

[a] E_1 is the potential for the semiquinone/hydroquinone couple, E_2 is the potential for the oxidized/semiquinone couple, and E_m is the potential for a 2-electron reduction. Data are given for solutions of flavodoxin in 50 mM K phosphate, pH 7, plus 0.3 mM EDTA, except for the wild type for which the buffer was 50 mM Na phosphate, pH 7. Wild-type and G61A mutant flavodoxins were reduced electrochemically while G61N, G61V, and G61L were reduced photochemically. Potentials were measured by potentiometry except in the case of G61N where potentials were determined by equilibration with the redox dye phenosaffranine and with hydrogen in the presence of catalytic amounts of hydrogenase. [b] Reference 24. [c] Reference 23. [d] Reference 21; data in brackets from ref 47.

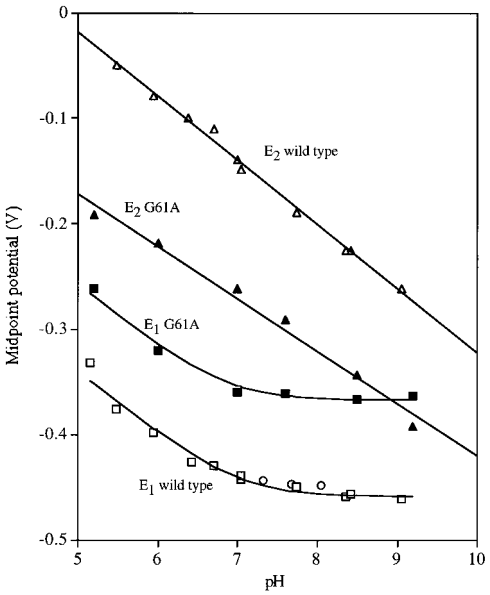

FIGURE 4: Effect of pH on the oxidation−reduction potentials of wild-type flavodoxin and the G61A mutant. Straight lines drawn through the points for E_2 are best-fit straight lines derived with the program MacCurveFit; curves drawn through the points for E_1 were fitted to the data using the equation $E_1 = E_B + (RT/F) \ln(1 + [H^+]/K)$ for a redox system in which there is a redox-linked protonation of the reductant with a dissociation constant K, and a limiting value E_B when the reductant is fully anionic and E_1 is independent of pH (*59*). The values determined for the apparent pK are 7.00 ± 0.11 (E_B = −0.458 V) and 6.84 ± 0.13 (E_B = −0.367 V) for the wild-type and G61A mutant, respectively. Data for the wild-type protein are from ref 24.

lization during the oxidation reaction than is observed during photoreduction when the semiquinone is stabilized thermodynamically.

The oxidation−reduction potentials associated with the two 1-electron steps in the reduction were determined for each mutant at pH 7 (Table 5), and in the case of the G61A mutant, measurements were also made at several pH values in the pH range 5.9−9.2 (Figure 4). The redox potentials for the two reduction steps of the G61A mutant are similar to those determined previously for the G61N mutant, and very different from those of wild-type flavodoxin. At pH 7.0 the value for E_2 is much more negative than that for the wild-type protein, while E_1 is 81 mV less negative. Much greater shifts in the two potentials occur with the valine and leucine mutants. However, the midpoint potential for the overall 2-electron reduction of the mutants is not too different from that of wild-type protein (a difference of +5 to −17 mV, depending on the mutant). The effect that the changes at glycine-61 have on the potentials, therefore, is to shift the potentials of the two 1-electron steps without much change to the overall midpoint potential.

Comparison of the redox potentials of the proteins with those of FMN in free solution is complicated because two rather different sets of data have been published for FMN (*21, 47*). The potential for the overall 2-electron reduction of wild-type flavodoxin and the mutant proteins is shifted on average about 90 mV to more negative values compared with the potential of free FMN. Similarly, the potential for the reduction of semiquinone to hydroquinone (E_1) is shifted to more negative values in all cases. Depending on which data set for free FMN is used for comparison, the change of E_2 when FMN is bound to the mutant proteins is either negative or positive. The difference between E_2 and E_1 is greater than that for free FMN, showing that thermodynamic stabilization of the semiquinone by the mutant proteins is greater than that which occurs with the free flavin.

The effects of pH on the potentials of the G61A mutant are similar to the effects on the potentials of the wild-type protein (Figure 4). The slope of the line drawn through the values for E_2 for the mutant is −50 mV/pH. This is less than the theoretical value of −59 mV/pH expected for the addition of one electron and one proton to the neutral oxidized flavin to give the neutral semiquinone at 25 °C, and it could indicate that a redox-linked pK_a is associated with the semiquinone form of this mutant. There was no evidence from the absorption spectrum for the formation of the anion of the flavin semiquinone, but the involvement of ionizable groups on the apoprotein cannot be excluded. The plot of E_1 versus pH for the mutant is a good fit to a theoretical curve in which a redox-linked protonation of the hydroquinone occurs at low pH and is associated with a pK_a of 6.84 ± 0.13. This apparent pK_a is similar to that calculated for wild-type flavodoxin (pK_a = 7.00 ± 0.11); the value for the wild-type protein is somewhat larger than the value reported earlier (pK_a = 6.8 (*24*)).

Flavin Binding by Mutant Apoflavodoxins. The binding of FMN and riboflavin by the mutant proteins was studied by removing the native flavin with trichloroacetic acid and then measuring the quenching of flavin fluorescence during stepwise addition of apoprotein to free flavin. Values for the dissociation constant of each complex were calculated from points in such titrations where free FMN was in equilibrium with bound FMN. The complexes with FMN are all very strong, but they are up to 10 times weaker than the complex with wild-type apoflavodoxin (Table 6). Similarly, while all of the mutant apoproteins form complexes with riboflavin, the complexes are up to 300 times weaker than the corresponding complex with wild-type protein. FMN is bound about 3000 times more tightly than riboflavin by wild-type apoprotein, indicating that the phosphate contributes a large fraction of the free energy of binding. Therefore interactions between the apoprotein and the isoalloxazine

Table 6: Dissociation Constants and Free Energies of Binding for Complexes of Wild-Type and Mutant Apoflavodoxins with Oxidized Riboflavin and the Three Redox Forms of FMN[a]

	riboflavin		FMN					
protein	K_d (mM)	ΔG_b (kcal mol^{-1})	$K_{d,ox}$ (nM)	$\Delta G_{b,ox}$ (kcal mol^{-1})	$K_{d,sq}$ (nM)	$\Delta G_{b,sq}$ (kcal mol^{-1})	$K_{d,hq}$ (μM)	$\Delta G_{b,hq}$ (kcal mol^{-1})
wild-type[b]	0.0051	−7.2	0.24 ± 0.1	−13.1 ± 0.3	0.006 ± 0.003	−15.3 ± 0.4	0.20 ± 0.12	−9.1 ± 0.5
G61N	0.2 ± 0.03 (8)	−5.03 ± 0.1	3.2[c]	−11.5	4.72[c]	−11.3	4.3[c]	−7.3
G61A	0.35 ± 0.02 (9)	−4.7 ± 0.1	0.82 ± 0.19 (5)	−12.3 ± 0.2	2.09 ± 0.8	−11.8 ± 0.3	3.02 ± 1.5	−7.5 ± 0.4
G61V	1.07 ± 0.16 (22)	−4.0 ± 0.1	2.4 ± 0.83(13)	−11.7 ± 0.3	97 ± 45	−9.5 ± 0.4	13.6 ± 7	−6.6 ± 0.5
G61L	0.33 ± 0.03 (10)	−4.7 ± 0.1	2.6 ± 0.11(12)	−11.7 ± 0.1	127 ± 30	−9.4 ± 0.2	20.1 ± 8	−6.4 ± 0.3

[a] Experiments were carried out in 50 mM K phosphate, pH 7, plus 0.3 mM EDTA at 25 °C except for the wild-type protein for which the buffer was 50 mM Na phosphate. The errors given are standard deviations. The value given in brackets after the error is the number of experimental points that was averaged. Dissociation constants for the reduced forms were calculated using the values for E_1 and E_2 of ref 21. The error given for the free energies of binding, ΔG_b, was calculated using the errors in the redox potentials and in the K_d values. [b] Data calculated from 24. [c] Data calculated from 23.

structure of the flavin must contribute a greater fraction of the total free energy of binding of riboflavin compared with FMN, and a mutation in the binding site that is near to the isoalloxazine evidently has a proportionately greater effect on the riboflavin complex than on the complex with FMN.

The redox potentials for the free and bound flavin can be used with the dissociation constant measured for the complex with oxidized flavin to calculate values for the dissociation constants for the complexes of apoflavodoxin with the two reduced forms of flavin (*24*). The calculations of Table 6 are based on the redox potentials for FMN determined by Draper and Ingraham (*21*). They show that although all three redox forms of FMN are bound more weakly by the mutant proteins than by wild-type apoflavodoxin, by far the greatest effect is on the complex with the flavin semiquinone. This is shown clearly when the dissociation constants for the different redox forms are used to calculate the free energies of binding (Table 6) according to eq 9:

$$\Delta G_b = -RT\ln(1/K_d) \quad (9)$$

where ΔG_b is the free energy for binding, R is the gas constant, and T is the temperature in degrees Kelvin, RT is 0.59 kcal at 25 °C, and K_d is the dissociation constant of the relevant complex. The plot of ΔG_b versus the three redox forms of the complexes (Figure 5) shows that the stabilities of the oxidized complexes of the mutants are not too different from that of the wild-type protein ($\Delta\Delta G_b^{ox} = 0.73$ to 1.5 kcal mol^{-1}). In addition, the hydroquinone complexes of the mutants have similar stabilities, and they are relatively little changed from the stability of the corresponding complex of wild-type flavodoxin ($\Delta\Delta G_b^{hq} = 1.6$ to 2.7 kcal mol^{-1}). In contrast, the stabilities of the semiquinone complexes are all less than those of the corresponding complexes with oxidized FMN, and very much less than that of the semiquinone of wild-type flavodoxin. The difference in the free energy of binding of the semiquinone by the wild-type protein and by the mutants G61A and G61N is 3.46 and 3.94 kcal mol^{-1}, respectively. The changes in binding energy for the two mutants with more bulky side chains are 5.72 and 5.88 kcal mol^{-1} for G61V and G61L, respectively.

Effects of Mutation at G61 on the Protein Structure. The overall conformations of the polypeptide chains of the four mutant proteins are very similar to that of wild-type flavodoxin. However, a marked difference occurs at the mutation site. Amino acid 61 is in a loop (the 60 loop) that

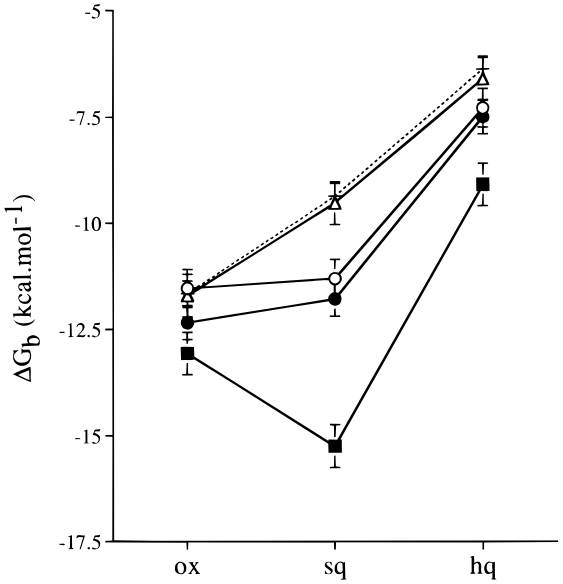

FIGURE 5: Variation of the free energy of binding of FMN to apoprotein with the redox state of the flavin. The data are from Table 3: (■), wild-type; (●), G61A; (○), G61N; (▽), G61V; (-+-), G61L.

contributes to the binding site for the isoalloxazine moiety of FMN. In all of the mutants, the loop is displaced by 5−6 Å away from the isoalloxazine structure (Figures 1 and 6). The changes in structure finish at Gln68 at which point the polypeptide chain rejoins the path taken in the wild-type protein. The conformational change in all of the mutants is such that the Cα−Cβ bond of the Ala, Val, Leu, or Asn side chains lies along the direction taken by the backbone N−Cα bond of Asp62 in the wild-type structure. The isoalloxazine moiety in the mutants is shifted approximately 0.2 Å in the plane of the ring system relative to that of the wild-type structure, a change that is close to the experimental error of the structures.

The large change in structure of the 60 loop in the mutants affects the hydrogen-bonding network at the FMN site (Figure 7). The program HBPLUS (*48*) was used to characterize the hydrogen-bonding networks in the wild-type and mutant proteins. The program calculates the positions of the hydrogen atoms and it uses both distance and angular criteria to determine whether a hydrogen-bonding interaction is possible. The calculations suggest that six hydrogen bonds are made between the isoalloxazine moiety in wild-type flavodoxin and either the protein or a water molecule. Five

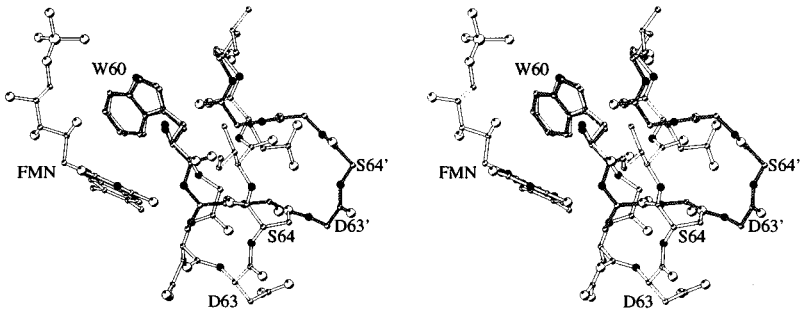

FIGURE 6: Stereoview of the least-squares superposition of the 60 loop of the G61A mutant (dark) onto the 60 loop of wild-type flavodoxin (light) using the Cα atoms of residues 2−59. Only the main chain atoms of the G61A 60 loop are shown for clarity. Nitrogen atoms are in black; C and O atoms are in gray, with larger radii assigned to oxygen. Residue labels or the G61A mutant are marked with an apostrophe. The figure was produced with the program MOLSCRIPT (*60*).

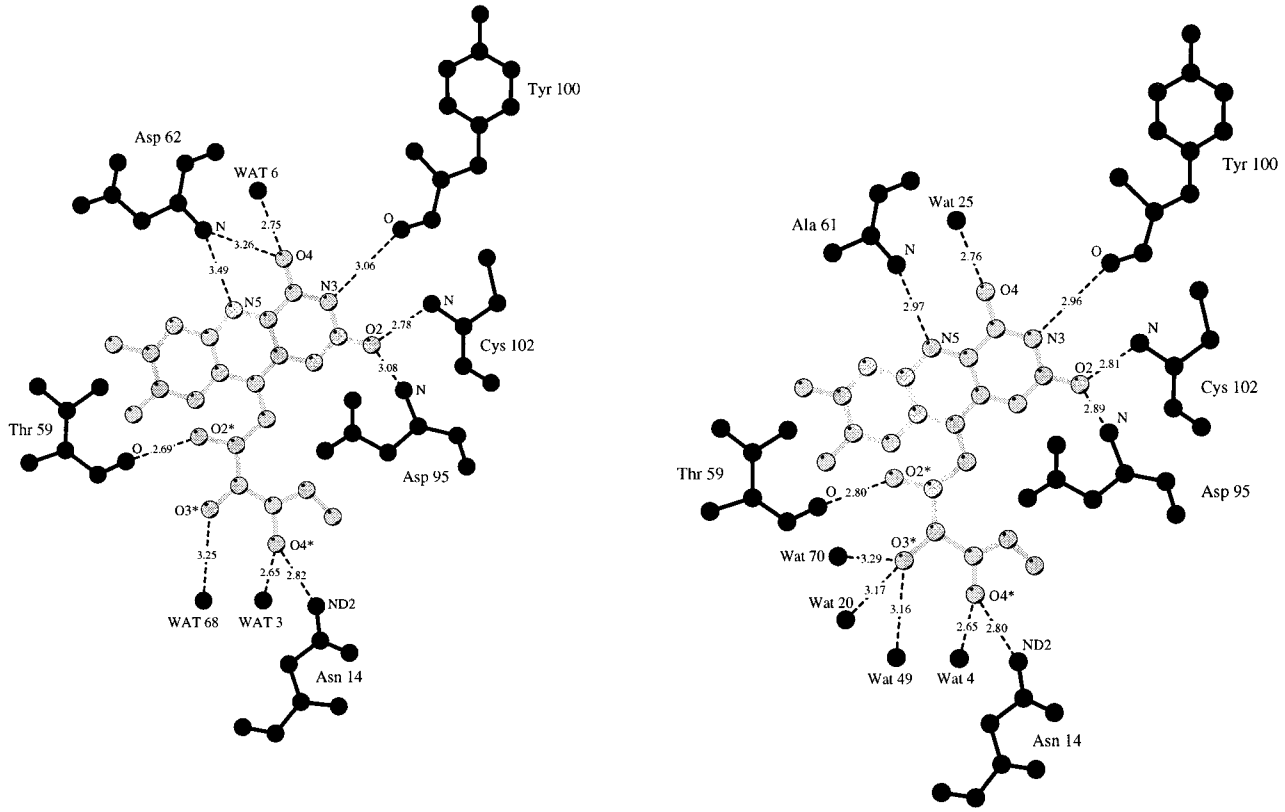

FIGURE 7: Hydrogen-bonding networks at the isoalloxazine binding site of (left) wild-type flavodoxin and (right) the G61A mutant. Hydrogen bonds are denoted by dashed lines, and distances are in angstroms. The figure was produced with the program LIGPLOT (*61*).

hydrogen bonds are formed with the isoalloxazine in the Gly61 mutants, and one of these also occurs to a water molecule. The largest differences between the hydrogen-bonding network of the mutants and the wild-type protein occur at the N(5) and O(4) atoms of the flavin. The conformation of the 60 loop in the mutants brings residue 61 into contact with the isoalloxazine, while in the structure of wild-type flavodoxin, Asp62 interacts with the flavin. It should be noted that the electron distribution of oxidized flavin, as determined by molecular orbital calculations, shows that N(5) is neutral (*49*) and a preferred site for nucleophilic addition (*50*). Therefore the hydrogen bond suggested by HBPLUS between N(5) and the backbone nitrogen of Asp62 in wild-type flavodoxin and Ala61 in the G61A mutant almost certainly does not occur. Further, the hydrogen bond that was identified earlier (*16*) between the backbone nitrogen of Asp95 and N(1) of the flavin is also unlikely to occur. The angles calculated between the hydrogen donor and the acceptor in this proposed bond are 122.5° and 118.4° for wild-type flavodoxin and the G61A mutant, respectively. These angles fall far from the ideal 180° angle for an optimal hydrogen-bonding interaction. In addition, the distance between the calculated hydrogen atom position and the acceptor atom in the wild-type protein is 2.6 Å, a value that is greater than the upper limit of 2.5 Å proposed for hydrogen bonds (*51*). The corresponding bond in the G61A mutant is 0.2 Å shorter due to the slight movement of the isoalloxazine structure. In summary, therefore, the hydrogen bond formed between the backbone nitrogen of Asp62 and O(4) of the isoalloxazine moiety in wild-type flavodoxin is the only one that is absent from the Gly61 mutant structures. Additional water molecules are found to interact with O(3)* of the ribityl side chain of FMN in the mutants. These were identified because the data for G61A were obtained to greater resolution than the data for the wild-type protein (*36*) and for the P2A pseudo-wild-type protein (*16*).

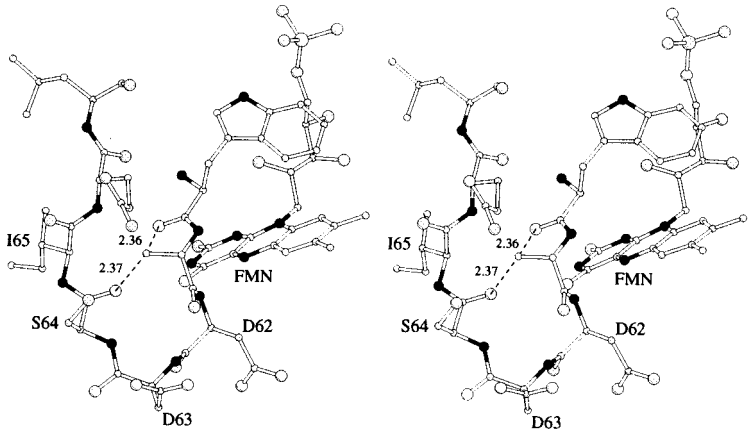

FIGURE 8: Stereoview of the 60 loop of wild-type flavodoxin with alanine modeled in place of glycine-61 to highlight the steric restraints imposed by adding a bulkier amino acid at this position. Nitrogen atoms are in black; C and O atoms are in gray, with larger radii assigned to oxygen. The figure was produced with the program MOLSCRIPT (*60*).

The mutations do not cause dramatic effects on the solvent accessibility of the atoms of the isoalloxazine moiety of the flavin. The use of a 1.4 Å spherical rolling probe (*52*) shows that the total exposure is approximately 104 Å^2 for the mutants and 94 Å^2 in wild-type flavodoxin. As was pointed out in an earlier study (*12*), the C7 and C8 methyl groups of the isoalloxazine moiety account for most of this accessible surface. For this reason, the large movement of the 60 loop in the Gly61 mutants does not significantly increase the overall solvent exposure of the isoalloxazine structure.

DISCUSSION

The observation that mutation of glycine-61 causes a selective destabilization of the complex of FMN semiquinone and apoflavodoxin from *D. vulgaris* provides support for the suggestion that the hydrogen bond between the backbone carbonyl of this residue and N(5)H of the half-reduced flavin is important in the regulation of the redox potentials of the bound flavin (*16*). In the oxidized form of this flavodoxin, the carbonyl group points away from the flavin. A conformational change in the protein on addition of an electron and a proton to the flavin causes the carbonyl to point toward the flavin and it brings the oxygen atom to 2.76 Å from N(5) (*16*). This conformation is preserved when a second electron is added to form the hydroquinone but the hydrogen bond is slightly longer (*16*). Our initial interpretation of the observation that the semiquinone is destabilized in the mutants was that the side chains of alanine, asparagine, valine, and leucine hinder the conformational change and make it more difficult for the carbonyl to hydrogen bond with N(5)H. However, the crystal structures of the oxidized forms of the mutant proteins make it clear that the changes in redox behavior cannot be explained simply by reference to the wild-type structure.

The large movement of the 60 loop in the mutants can be rationalized by the steric constraints at the mutation site. The conformation of the 60 loop in *D. vulgaris* flavodoxin is such that mutation of Gly61 even to alanine results in unfavorable contacts between the additional Cβ atom and the carbonyl oxygens of Trp60 and Ser64 (Figure 8). The doubling back of the loop in this flavodoxin allows only glycine at position 61. A torsion which moves the Cβ of the amino acid at position 61 toward Asn62 relieves the steric strain. This movement forces the movement of Asp62, a residue that is hydrogen-bonded to O(4) of the flavin. However, the movement of the loop observed in the mutant proteins is much larger than might be expected to relieve steric strain. The large displacement is probably driven by a combination of steric relief and the need to replace the hydrogen bonds broken during the structural reshuffling. This is in stark contrast to the situation in flavodoxin from *C. beijerinckii* in which the glycine residue that is equivalent to Gly61 in *D. vulgaris* flavodoxin can be mutated to various amino acids with little or no change in protein structure (*53*). The structure of the flavin-binding site of *C. beijerinckii* flavodoxin is such that no steric strain is imposed when Gly57 is mutated to Ala, Asn, or Asp. Only on mutation to threonine is any significant change in structure observed, and even then it is small in comparison with the changes observed with *D. vulgaris* flavodoxin. Further, in *C. beijerinckii* flavodoxin the equivalent glycine-aspartate peptide may adopt three conformations: trans-O up in which the carbonyl oxygen of Gly57 points toward the flavin (similar to the semiquinone structure of *D. vulgaris* flavodoxin); trans-O down in which the O(57) points away from the flavin (equivalent to the oxidized structure of *D. vulgaris* flavodoxin); and cis-O down, a structure that is unique to this flavodoxin. The last of these conformations is stabilized in the crystal structure by an intermolecular hydrogen bond to Asn137. In the absence of this hydrogen bond the trans-O down conformation predominates in the mixture of conformational states. Since the three conformations occur as a mixture in oxidized *C. beijerinckii* flavodoxin, it is concluded that the energy barriers between them must be small (*53*). The flavin-binding site of *D. vulgaris* flavodoxin differs such that it allows the subtle conformation change and hydrogen-bonding interaction of the carbonyl of Gly61 and N(5)H of the flavin semiquinone to occur. The observation that the displacement of the 60 loop in the oxidized structure is essentially identical when Gly61 is mutated to Ala, Asp, Val, or Leu points to the pivotal role of this conserved glycine residue. The 60 loop in wild-type flavodoxin from *D. vulgaris* is longer by two amino acids than the corresponding loops in other flavodoxins. This added length in combination with the glycine residue at the start of the loop may give the *D. vulgaris* protein additional flexibility for interaction with other redox proteins. Evidence for greater than expected flexibility in this loop has come from NMR spectroscopy

Table 7: Intermolecular Hydrogen Bonds in the Crystal Structures of Wild-Type Flavodoxin and the G61A Mutant

	atom 1	atom 2	symmetry operator[a]	distance (Å)
wild-type flavodoxin[b]			$P4_32_12$	
	Gly61-N	Asp28-O	I	2.68
	Ile65-N	Arg131-O	II	2.81
	Glu66-OE_2	Arg145-NH1	I	3.04
G61A mutant flavodoxin			$P2_12_12$	
	Asp63-O	Tyr17-OH	III	2.68
	Asp63-O	Arg134-NE	III	2.81
	Ser64-O	Arg134-NH2	III	2.90

[a] Symmetry codes (I) 1/2-Y, X-1/2, Z-1/4; (II) X-1/2, 1/2-Y, 1/4-Z; (III) X, Y, Z+1. [b] Data from structure refined to 1.7 Å resolution (M. A. Walsh, unpublished results).

(*54*, *55*) and from the X-ray crystal structures of additional mutants (*35*, *56*).

Analysis of the intermolecular contacts in the crystal structure of wild-type *D. vulgaris* flavodoxin shows that the 60 loop is stabilized by three hydrogen bonds to other molecules in the unit cell (Table 7). The crystal packing of the Gly61 mutants is less tight than that which occurs with wild-type flavodoxin, but again three possible intermolecular hydrogen bonds occur (Table 7). However, it must be stressed that the changes in structure observed in the Gly61 mutants are more likely to be a consequence of the steric restraints imposed by the mutation than by the different crystal packing arrangements of the mutants. In other words, the structural changes cause the different packing and space group symmetry of the crystals of the mutant proteins. It is interesting, however, that the new structures suggest the possibility that there are alternative solution structures for both the mutants and wild-type proteins. The influence of intermolecular contacts on the conformation of the 60 loop is hard to assess from the crystallographic data alone. If these interactions do play a significant role, then in the case of the wild-type oxidized crystal structure it would be reasonable to argue that the unfavorable backbone ϕ and ψ angles are due to the intermolecular interactions in the crystal rather than being imposed by the protein structure to provide the optimal conformation for the peptide flip that occurs at Gly61 when the flavin is reduced. The conformation of the 60 loop in the Gly61 mutants is such that a far more complex structural change is required to form a similar hydrogen-bonding interaction with the protonated N(5) of the reduced flavin. NMR analyses of these mutants should provide important information that could be used to further assess the influence of intermolecular interactions in the crystal structures reported here and on the importance of the 60 loop in modulating the redox potentials of FMN.

The changes in structure and in the hydrogen-bonding pattern observed for the mutants compared with the oxidized form of wild-type flavodoxin are presumably responsible for the decrease in affinity of the mutants for oxidized FMN (average change about 1 kcal mol^{-1}; Table 4). However, the structural changes in oxidized flavodoxin indicate that if a hydrogen bond forms between the carbonyl of residue 61 and N(5)H of the flavin semiquinone in the mutants, the conformational change required must be more complex than that occurring in the wild-type protein. Attempts to determine the structures of the reduced forms of the Gly61 mutant proteins have met with only partial success. When crystals of the mutants are treated with dithionite ion, the yellow oxidized flavin is bleached, indicating that the flavin is reduced, but the crystals usually rapidly crack and disintegrate. A small platelike crystal of the G61A mutant ($0.4 \times 0.2 \times 0.1$ mm^3) survived this treatment at pH 7 and changed from yellow-orange, typical of oxidized flavodoxin, to purplish-red, as expected for flavodoxin semiquinone. X-ray diffraction data were collected to 2.5 Å. The resulting electron density was interpretable except in the region of residues 61−65. The poor electron density in this region might indicate that the crystal contained a mixture of oxidation states, since only 80% conversion to the semiquinone occurs on addition of one reducing equivalent in solution. However, the extent of the disorder suggests that a large change in structure might have occurred. The observed disintegration of most crystals of the mutants on reduction also points to a change in conformation that is too large to be accommodated by the crystal packing. The conformational change that occurs when wild-type flavodoxin is reduced is probably driven by the interaction between N(5) of the flavin and the NH of Asp-62 which is 3.6 Å away (*16*). In the absence of a conformational change, protonation at N(5), as occurs in the reduced forms of the flavin, would result in an unfavorable H−H interaction. The distance between N(5) and the NH of residue 61 in the mutant proteins is about 3 Å (*56*) with the result that protonation at N(5) would also result in strong unfavorable interactions in the absence of a conformational change to move the two groups apart. Further, the pH study showed that the G61A mutant stabilizes the neutral form of the semiquinone even at pH 9.2, a pH value above the pK_a of the flavin N(5)H in free solution. The shift in pK_a suggests that a hydrogen bond is formed to N(5)H, and in the absence of a suitable acceptor nearby in the structure of the oxidized protein, a conformational change is necessary to supply a group to which N(5)H can hydrogen bond in the reduced protein. It is nevertheless interesting that the difference in free energy of binding of the FMN semiquinone by this mutant and by wild-type flavodoxin is slightly less than the free energy of a hydrogen bond (5 kcal mol^{-1} (*57*)) while the difference in binding energies for G61V and G61L are similar to the energy of a hydrogen bond.

This study was initiated to investigate the role of the redox-linked conformational change at Gly61 in modulating the redox potentials of the bound FMN in flavodoxin. The thermodynamic properties of the mutants show the expected trend: lengthening the side chain at position 61 destabilizes the semiquinone. However, the crystallographic work shows that this result cannot be interpreted simply by reference to the wild-type structure. The structural changes observed on mutation demonstrate the flexibility of the 60 loop, while

the differences between the mutant and wild-type structures indicate that the redox-linked conformational change, which we assume to occur in the mutants, must be different from that occurring in the wild-type protein. The large structural perturbation of the 60 loop that results from mutation of one amino acid shows that caution is necessary in the interpretation of such mutagenesis studies.

REFERENCES

1. Mayhew, S. G., and Ludwig, M. L. (1975) in *The Enzymes* (Boyer, P., Ed.) 3rd ed., Vol. 12, pp 57−109, Academic Press, New York.
2. Mayhew, S. G., and Tollin, G. (1992) in *Chemistry and Biochemistry of Flavoenzymes* (Müller, F., Ed.) vol. 3, 389−426, CRC Press, Boca Raton, Florida.
3. Ludwig M. L., and Luschinsky, C. L. (1992) in *Chemistry and Biochemistry of Flavoenzymes* (Müller, F., Ed.) Vol. 3, 427−466, CRC Press, Boca Raton, Florida.
4. Ludwig, M. L., Schopfer, L. M., Metzger, A. L., Pattridge, K. A., and Massey, V. (1990) *Biochemistry 29*, 10364−10375.
5. Franken, H.-D., Rüterjans, H., and Müller, F. (1984) *Eur. J. Biochem. 138*, 481−489.
6. Vervoort, J., Müller, F., Mayhew, S. G., van den Berg, W. A. M., Moonen, C. T. W., and Bacher, A. (1986) *Biochemistry 25*, 6789−6799.
7. Vervoort, J., Müller, F., LeGall, J., Bacher, A., and Sedlmaier, H. (1985) *Eur. J. Biochem. 151*, 49−57.
8. Stockman, B. J., Westler, W. M., Mooberry, E. S., and Markley, J. L. (1988) *Biochemistry 27*, 136−142.
9. Swenson, R. P., and Krey, G. D. (1994) *Biochemistry 33*, 8505−8514.
10. Zhou, Z., and Swenson, R. P. (1995) *Biochemistry 34*, 3183−3192.
11. Zhou, Z., and Swenson, R. P. (1996) *Biochemistry 35*, 12443−12454.
12. Zhou, Z., and Swenson, R. P. (1996) *Biochemistry 35*, 15980−15988.
13. Moonen, C. T. W., Vervoort, J., and Müller, F. (1984) *Biochemistry 23*, 4859−4867.
14. Zheng, Y.-J., and Ornstein, R. L. (1996) *J. Am. Chem. Soc. 118*, 9402−9408.
15. Smith, W. W., Burnett, R. M., Darling, G. D., and Ludwig, M. L. (1977) *J. Mol. Biol. 117*, 195−225.
16. Watt, W., Tulinsky, A., Swenson, R. P., and Watenpaugh, K. D. (1991) *J. Mol. Biol. 218*, 195−208.
17. Luschinsky, C. L., Dunham, W. R., Osborne, C., Pattridge, K. A., and Ludwig, M. L. (1991) in *Flavins and Flavoproteins 1990* (Curti, B., Ronchi, S., and Zanetti, G., Eds.) 409−414, de Gruyter, Berlin.
18. Romero, A., Caldiera, J., LeGall, J., Moura, I., Moura, J. J. G., and Romao, M. J. (1996) *Eur. J. Biochem. 239*, 190−196.
19. van Mierlo, C. P. M., Lijnzaad, P., Vervoort, J., Müller, F., Berendsen, H. J. C., and de Vlieg J. (1990) *Eur. J. Biochem. 194*, 185−198.
20. Sharkey, C., Mayhew, S. G., Higgins, T. M., and Walsh, M. A. (1997) in *Flavins and Flavoproteins 1996* (Stevenson, K. J., Massey, V., and Williams, C. H., Jr., Eds.) pp 445−448, University of Calgary Press, Calgary.
21. Draper, R. D., and Ingraham, L. Y. (1968) *Arch. Biochem. Biophys. 125*, 802−808.
22. Laudenbach, D. E., Straus, N. A., Pattridge, K. A., and Ludwig, M. L. (1987) *Flavins and Flavoproteins 1987* (Edmonson, D. E., and McCormick, D. B., Eds.) pp 249−260, de Gruyter, Berlin.
23. Carr, M. C., Curley, G. P., Mayhew, S. G., and Vordouw, G. (1990) *Biochem. Int. 20*, 1025−1032.
24. Curley, G. P., Carr, M. C., Mayhew, S. G., and Voordouw, G. (1991) *Eur. J. Biochem. 202*, 1091−1100.
25. Kunkel, T. A., Roberts, J. D. and Zakour, R. A. (1987) *Methods Enzymol. 154*, 367−382.
26. Sanger, F., Nicklen, S., and Coulson, A. R. (1977) *Proc. Natl. Acad. Sci. U.S.A. 74*, 5463−5467.
27. Kleiner, D., Wyatt, P., and Merrick, M. J. (1988) *J. Gen. Microbiol. 134*, 1779−1784.
28. Sambrook, J., Fritsch, E. F., and Maniatis, T. (1989) *Molecular Cloning: A Laboratory Manual*, 2nd ed., Cold Spring Harbor Laboratory Press, Cold Spring Harbor, New York.
29. Pueyo, J. J., Curley, G. P., and Mayhew, S. G. (1996) *Biochem. J. 313*, 855−861.
30. Wassink, J. M., and Mayhew, S. G. (1975) *Anal. Biochem. 68*, 609−616.
31. Massey, V., and Hemmerich, P. (1978) *Biochemistry 17*, 9−16.
32. Stankovich, M. (1980) *Anal. Biochem. 109*, 295−308.
33. Clark, W. M. (1960) *Oxidation Reduction Potentials of Organic Systems*, The Williams and Wilkins Co., Baltimore.
34. Michaelis, L. (1932) *J. Biol. Chem. 96*, 703−715.
35. Walsh, M. A. (1994) Ph.D. Thesis, National University of Ireland.
36. Watenpaugh, K. D., Sieker, L. C., Jensen, L. H., LeGall, J., and Dubourdieu, M. (1972) *Proc. Natl. Acad. Sci. U.S.A 69*, 3185−3188.
37. Ducruix, A., and Giege, R. (1992) *Crystallization of nucleic acids and proteins*, IRL Press, Oxford.
38. Otwinowski, Z., and Minor, W. (1997) *Methods Enzymol. 276*, 307−326.
39. Fitzgerald, P. M. D. (1988) *J. Appl. Crystallogr. 21*, 273−278.
40. Collaborative Computational Project, No. 4 (1994) *Acta Crystallogr. D50*, 760−763.
41. Hendrickson, W. A., and Konnert, J. H. (1980) in *Computing in Crystallography* (Diamond, R., Ramaseshan, R., and Venkatesan, K., Eds.) Chapter 13, pp 1−23, The Indian Academy of Sciences, Bangalore.
42. Lamzin, V. S., and Wilson, K. S. (1997) *Methods Enzymol. 277*, 269−305.
43. Brünger, A. T. (1992) *Nature 355*, 472−475.
44. Jones, T. A., Zou, J. Y., Cowan, S. W., and Kjeldgaard, M. (1991) *Acta Crystallogr. A47*, 110−119.
45. Ramachandran, G. N., and Sasisekharan, V. (1968) *Adv. Protein Chem. 23*, 283−437.
46. Bernstein, F. C., Koetzle, T. F., Williams, G. J. B., Meuer, E. F. J., Brice, M. D., Rodgers, J. R., Kennard, O., Shimanouchi, T., and Tasumi, M. (1977) *J. Mol. Biol. 112*, 535−542.
47. Anderson, R. F. (1983) *Biochim. Biophys. Acta. 772*, 158−162.
48. McDonald, I., and Thornton, J. (1994) *J. Mol. Biol. 238*, 777−793.
49. Hall, L., Orchard, B., and Tripathy, S. (1987) *Int. J. Quantum Chem. 31*, 217−242.
50. Müller, F., and Massey, V. (1969) *J. Biol. Chem. 244*, 4007−4016.
51. Baker, E. N., and Hubbard, R. E. (1984) *Prog. Biophys. Mol. Biol. 44*, 97−179.
52. Connolly, M. L. (1983) *Science 221*, 709−712.
53. Ludwig, M. L., Pattridge, K. A., Metzger, A. L., Dixon, M. M., Eren, M., Feng, Y., and Swenson, R. P. (1997) *Biochemistry 36*, 1259−1280.
54. Knauf, M. A., Löhr, F., Blümel, M., Mayhew, S. G., and Rüterjans, H. (1996) *Eur. J. Biochem. 238*, 423−434.
55. Hrovat, A., Blümel, M., Löhr, F., Mayhew, S. G., and Rüterjans, H. (1997) *J. Biomol. NMR 10*, 53−62.
56. McCarthy, A. A. (1997) Ph.D. Thesis, National University of Ireland.
57. Fersht, A. (1985) *Enzyme structure and mechanism*, p 298, Freeman and Co., New York.
58. Laskowski, R. A., MacArthur, M. W., Moss, D. S., and Thornton, J. M. (1993) *J. Appl. Crystallogr. 26*, 283−291.
59. Mayhew, S. G., Foust, G. P., and Massey, V. (1969) *J. Biol. Chem. 244*, 803−810.
60. Kraulis, P. J. (1991) *J. Appl. Crystallogr. 24*, 946−950.
61. Wallace, A. C, Laskowski, R. A., and Thornton, J. M. (1995) *Protein Eng. 8*, 127−134.

BI973193K